Beam-Based Lattice Topology Transition With Function Representation

Nikita Letov, Yaoyao Fiona Zhao

Beam-based lattice topology transition with function representation

Nikita Letov
Department of Mechanical Engineering
McGill University
Montréal, QC H3A 0G4, Canada
Email: nikita.letov@mail.mcgill.ca

Yaoyao Fiona Zhao*
Department of Mechanical Engineering
McGill University
Montréal, QC H3A 0G4, Canada
Email: yaoyao.zhao@mcgill.ca

A lattice structure is a porous periodic structure with unit cells organized according to a pattern. Lattice structures are lightweight parts that are commonly produced by additive manufacturing techniques. Lattice structures require their topology defined which effectively defines the connectivity of their unit cell. Many of these topologies are beam-based, i.e. their unit cell is represented by a network of nodes connected with beams. Such lattice structures require a geometric modeling tool capable of generating their solid model. This paper presents a method to support the topology transition for beam-based lattice structures by controlling the geometric parameters of topologies. This control is made possible with the function representation of the geometry. The work also analyzes how suitable different beam-based lattice topologies are to support the transition. A few case studies are carried out to demonstrate the feasibility of the proposed method.

NOMENCLATURE

3D three-dimensional
AM additive manufacturing
ASCII American Standard Code for Information Interchange
B-rep boundary representation
BCC body-centered cubic
BCCz body-centered cubic with additional 4 z-direction oriented beams
CAD computer-aided design
CPU central processing unit
DFAM design for additive manufacturing
F-rep function representation
FBCC face- and body-centered cubic
FCC face-centered cubic
FCCz face-centered cubic with additional 4 z-direction oriented beams
FOSS free and open-source software
GMK geometric modeling kernel
GPU graphics processing unit
OCCT Open CASCADE Technology
RAM random-access memory
S-FBCCz self-supporting face-centered cubic without horizontal beams with additional 4 z-direction oriented beams
S-FCC self-supporting face- and body-centered cubic without horizontal beams
S-FCCz self-supporting face-centered cubic without horizontal beams with additional 4 z-direction oriented beams
STL stereolithography
SSD solid-state drive
TPMS triply periodic minimal surface

1 INTRODUCTION

Ever since its introduction, additive manufacturing (AM) has been able to push the manufacturing freedom to the new frontiers. AM has found its application in part consolidation, rapid prototyping, and manufacturing of geometrically complex and hollow structures [1, 2, 3].

Lattice structures are an example of a complex geometric object that can be produced with AM. Some lattice structures can be manufactured with subtractive manufacturing techniques [4]. However, more geometrically complex lattice structures, such as heterogeneous and multi-scale lattice structures, often require AM for their manufacturing. Lattice structures provide increased strength-

*Corresponding author.

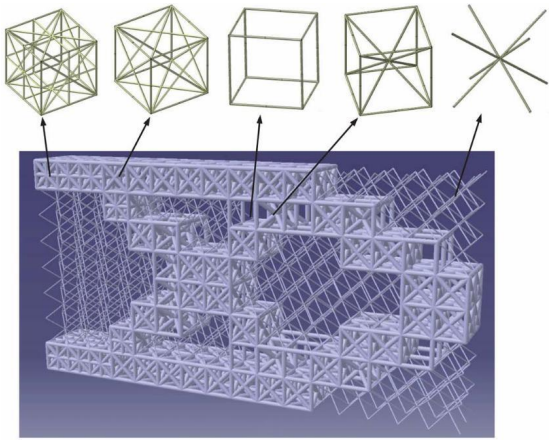

Fig. 1: An example of a lattice structure with multiple topologies that are inspired by topology optimization [12]

to-weight ratio without a significant decrease of strength properties [5]. Moreover, other physical and mechanical properties which are different from their parent material can emerge in a lattice structure [6, 7]. Lattice structures can be classified to be either homogeneous or heterogeneous. Homogeneous lattice structures have their topology and geometric parameters constant across the structure, while heterogeneous lattice structures have varying topologies or geometric parameters. Geometric and mechanical properties of lattice structures have secured their place in such industries as aerospace [7], automotive [8], prosthetics [9], and more [10].

A lattice structure with multiple homogeneous regions is an example of a heterogeneous lattice structure. Different topologies have different mechanical properties in different directions [11]. Assigning various topologies to different regions of the same structure ensures the variation of mechanical properties within that structure. This effect is often utilized in design for additive manufacturing (DFAM) [12]. For example, topology optimization can often be used to identify the optimal topology for each unit cell of a lattice depending on the loading conditions [13, 14]. Figure 1 illustrates an example of a lattice structure with topologies selected based on a topology optimization algorithm.

Geometric modeling of lattice structures has been a challenge in AM due to the inability of conventional tools to model periodic structures [15]. Even more challenging is geometric modeling of heterogeneous lattice structures [16].

While AM continuously allows manufacturing of an ever-increasing variety of lattice structures [17], the design freedom is still limited for the design of lattice structures. Such limitation is often associated with the geometric modeling functionality of the existing computer-aided design (CAD) tools for lattice structures [15]. Conventional CAD tools which are based on features are well-suited for subtractive manufacturing but fail to provide sufficient design flexibility when modeling complex periodic structures [16].

There is a research gap between manufacturing freedom and design freedom that is yet to be crossed from both sides. First, not all designed parts can be manufactured and the manufacturing freedom is thus limited [18]. Second, not everything that is manufactured can be easily modeled, which is a gap that can be crossed by future developments in geometric modeling for AM and that has been identified in the literature [15]. This gap can be crossed by providing an appropriate geometric modeling approach that would allow efficient and convenient control over the geometric parameters and the topology of a lattice structure.

The topic of topology transition in lattice structures is not a new one [19]. Geometric modeling of transition between areas with different topologies within the same lattice structure is of particular interest in research on this topic. A smooth transition between topologies that are arbitrarily oriented between each other finds its application in, for example, the design of bone implants [20]. Trabecular bone has multiple porous microstructures which are oriented depending on the direction the load which is commonly applied to the bone. The regions of the bone which are subject to the same type of load possess similar mechanical properties which are achieved by a seemingly randomized natural lattice structure with arbitrarily oriented beams.

This paper presents the research work that is a direct continuation of a previously published work that was focused on providing a framework for functional control over the geometric parameters of a lattice structure [21]. The purpose of this paper is to analyze the possible combinations of beam-based topologies within a single lattice and extend the previously developed framework to enable functional control over the topology in it. Figure 2 illustrates various ways of enabling heterogeneity of lattice structures with the main topic of this paper highlighted in bold. To summarize, this paper attempts to provide a methodology that can be applied in the geometric modeling of beam-based lattice structures with multiple topologies. Note that even though material heterogeneity is a noticeable topic of interest in the research on lattice structures [22], this paper focuses only on the geometric aspect of modeling.

The proposed paper does not focus on topology optimization itself However, the proposed method can be

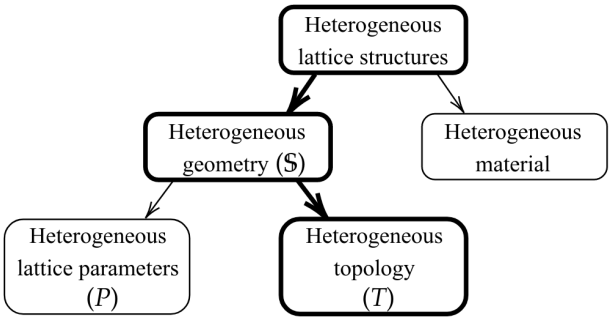

Fig. 2: Various ways to parametrize heterogeneous lattice structures with the direction chosen for this paper encircled with bold lines

eventually applied to topology optimization. For example, it has been shown that if a solid body is defined as with function representation, then the optimization of the arguments of the underlying function results in a topologically optimized structure [23].

Even though surface-based topologies such as the topologies based on the triply periodic minimal surfaces (TPMS) are a topic of interest in the research on topology transition [24, 25]. This paper only focuses on the beam-based lattice topologies.

The rest of this paper is organized as follows. Section 2 reviews the literature on the existing geometric modeling methods that support AM of lattice structures with multiple topologies. Section 3 describes the method that is proposed to be used as a support for the geometric modeling of lattice structures with multiple topologies. Section 4 documents the technical aspects of the implementation, as well as provides several use cases of lattice structures modeled with the proposed approach. The conclusions and directions of future research are provided in section 5.

2 GEOMETRIC MODELING OF MULTI-TOPOLOGY BEAM-BASED LATTICE STRUCTURES

Normally, the unit cells in lattice structures are aligned in a three-dimensional (3D) pattern in which every two neighboring unit cells share a side. This work, however, focuses on the geometric modeling of more unconventional methods of aligning the unit cells. This includes the modeling of lattice structures in which the topologies are aligned at an angle to each other, as well as the variation of topologies that is ensured by the variation of geometric parameters.

The rest of this section is organized as follows. Concepts that are relevant to the geometric modeling of lattice structures are reviewed in section 2.1. Section 2.2 reviews the function representation (F-rep) methods that are applicable to the geometric modeling of lattice structures. One of the main challenges that were identified in the literature corresponds to the so-called *connectivity issue* which is introduced in detail in section 2.3.

2.1 Geometric modeling concepts

The geometric modeling of lattice structures has been extensively reviewed in the literature [15, 16, 26]. Similarly to every CAD tool, any lattice modeling tool has a geometric modeling kernel (GMK) at its core. A GMK is a software representation of a set of geometric theorems and axioms that is crucial to defining the shape of a solid body.

While multi-topology beam-based lattice structures have been a topic of interest in AM research, the geometric modeling methods used to generate their respective solid models are limited [27]. The literature review performed in the preceding works has revealed that not many tools allow variation of geometric parameters other than the thickness of the lattice beams [15, 21].

In this work, the solid model $\mathbb{S} \subset \mathbb{R}^3$ is defined in the 3D design space $\mathbf{X} \subset \mathbb{R}^3$ as a set of points bounded by its boundary surface $\partial\mathbb{S}$ which is defined as

$$\partial\mathbb{S} := \overline{\mathbb{S}} \cap \overline{(\mathbf{X} - \mathbb{S})} \tag{1}$$

and is a 2-manifold M_g^2 of a finite genus g. The design space $\mathbf{X}$ is considered to be defined by the design and environment constraints.

Consider that the boundary surface is defined by a function $F(\mathbf{X})$ such that all $\mathbf{X}$ satisfying $F(\mathbf{X}) \geq 0$ lie inside the solid body. Then,

$$\mathbb{S} := \{\mathbf{X} | F(\mathbf{X}) \geq 0\} \tag{2}$$

and Eqn. (1) converges to

$$\partial\mathbb{S} = \{\mathbf{X} | F(\mathbf{X}) = 0\}. \tag{3}$$

Geometric modeling in general can be classified into surface and volumetric modeling. Surface modeling represents a solid body solely by its surface boundary. The most common way of surface modeling is based on boundary representation (B-rep) in which only $\partial\mathbb{S}$ is required to be defined, i.e. all points satisfying $F(\mathbf{X}) = 0$

are required to be modeled. Similarly, volumetric modeling requires finding a solution for $F(\mathbf{X}) \geq 0$. The key differences and advantages of both approaches are covered in the preceding works [15, 28].

2.2 Function representation applicability for geometric modeling of beam-based lattice structures

Geometric modeling approaches that define the geometric shape of the target solid body by providing either an explicit or an implicit form of $F(\mathbf{X})$ are called the F-rep methods [29]. F-rep is a powerful approach that allows direct control over the shape of the desired solid body given that its shape can be described by a mathematical equation. In F-rep, a solid body is defined by the inequality

$$F(\mathbf{X}) \geq 0, \tag{4}$$

where $X = (x, y, z) \subset \mathbb{R}^3$ is the design space and $F(\mathbf{X})$ is defined in such a way, that $F(\mathbf{X}) \geq 0$ is the solid itself, $F(\mathbf{X}) = 0$ corresponds to the surface of the solid, and $F(\mathbf{X}) < 0$ is the rest of the design space [29].

Moreover, F-rep has proved itself applicable for the geometric modeling of heterogeneous lattice structures [21]. This is achieved by expanding the classical F-rep definition of geometry defined by Eqn. 4 by composing it of a function $P(\mathbf{X})$ that defines the geometric parameters of the lattice unit cells and a function that defines the topology $T(\mathbf{X})$ of the lattice, i.e.

$$F(\mathbf{X}) = (P \circ T)(\mathbf{X}) \geq 0. \tag{5}$$

Figure 3 illustrates the sequential mapping described by Eqn. (5). Note that the order of the composition matters. First, the topology of the whole multi-topology lattice is defined by the mapping $t = T(\mathbf{X})$, where $t \in \mathbb{Z}^3$ is a scalar integer space that describes the distribution of topologies in the design space $\mathbf{X}$. t is discrete because the set of unit cells is a countable set, i.e. each unit set can be assigned a finite number. No topology at a certain $x \in \mathbf{X}$ is a case of 0-topology where no geometry exists. These points x, however, lie outside the solid where $F(\mathbf{X}) < 0$ and are thus redundant to be defined. Then, the geometric parameters of every region of the lattice are applied to the topology by the mapping $p = P(t)$. If p is a geometric parameter and $F = p - T(\mathbf{X})$, then $P(T(\mathbf{X}))$ is a trivial function, and the resulting lattice structure is equivalent to its skeletal graph with the 0-thickness, or T. In general, $p \in \mathbb{R}^g$ where g is the number of geometric parameters required to define a solid model of a lattice unit cell. For

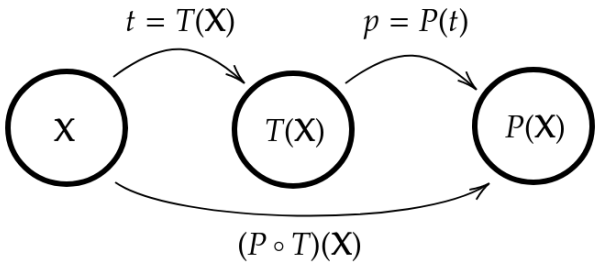

Fig. 3: The mapping of the function T that defines the topology and the function P that defines the geometric parameters of a single heterogeneous lattice structure

example, the lattice thickness and the unit cell size can be parameters that are needed to fully define the solid model of a unit cell. Functions P and T define two different aspects of the heterogeneous geometry of a lattice structure as shown in Fig. 2. The mathematical foundations of this approach are described in more details in the preceding work [21].

This approach allows setting a constant topology T and a custom set of geometric parameters P. Topology in this approach is defined by its skeletal graph which is a set of straight line segments which are defined by mathematical equations and intersect at nodes. In other words, a skeletal graph is a single unit cell with the 0 thickness of beams. For example, a topology defined by

$$T(\mathbf{X}) : \begin{cases} \begin{bmatrix} x \in \{0, u\}, z \in \{y, -y + u\}, \\ y \in \{0, u\}, z \in \{x, -x + u\}, \\ z \in \{0, u\}, y \in \{x, -x + u\}; \end{bmatrix} \\ x, y, z \in [0, u], \end{cases} \tag{6}$$

where u is the side of the cubic unit cell, describes 12 straight line segments bounded by the cubic region $x, y, z \in [0, u]$ with each segment being from one vertex to the opposite one within the same face of the cube. In this notation, $\alpha \in \{\beta, \gamma\}$ means a union of $\alpha = \beta$ and $\alpha = \gamma$. So, $x \in \{0, u\}$ means $x = 0$ and $x = u$. Eqn. (6) describes the skeletal graph of the FCC topology which is sketched in Fig. 4.

The definition of the geometric parameter function P allows adding thickness and other geometric parameters to the skeletal graph, thus enabling the modeling of solid bodies. Figure 5 shows some of the topologies inspired by the metal crystal structure and which are supported by default in this approach. All the illustrated unit cells have the unit cell size $u = 10$ mm, the beam diameter $d = 1$ mm, and the node diameter $D = 1.1$ mm. Note

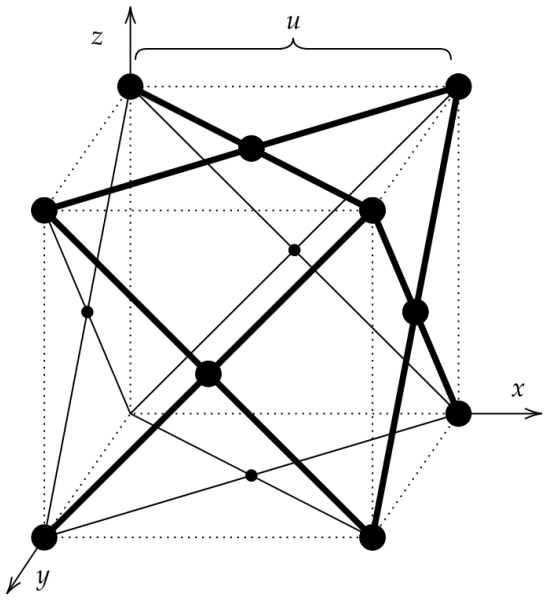

Fig. 4: An FCC unit cell described by Eqn. (6). The thicker lines correspond to the beams that are located in visible faces of the arbitrary cube with the side u. The edges of the arbitrary cube are represented as dotted lines. The nodes are represented as circles.

that the FCC topology observed in Fig. 5a is obtained by adding the thickness parameter to the skeletal graph defined by Eqn. (6) and illustrated in Fig. 4. Figure 6 illustrates other beam-based topologies that are supported by the approach. Note that the rhombicuboctahedron and the truncated cube topologies can optionally require the truncation size parameter as they are based on truncated polyhedrons. These unit cells have the unit cell size $u = 10$ mm, the beam diameter $d = 1$ mm, and the node diameter $D = 1.1$ mm.

F-rep is a powerful geometric modeling technique that greatly expands the complexity of the solid models it can produce [30]. This method, however, introduces additional complexity to the design process itself by providing more complex tools to model solid bodies. The advantage of the method that is proposed to be used in this work lies in its simplification of the F-rep for the modeling of lattice structures. The software implementation of the approach that has been released as a free and open-source (FOSS) software [31] has a list of predefined topology functions T with the ability to extend them at will. For instance, Eqn. (6) is essentially simplified to $T(\mathbf{X}) : FCC(\mathbf{X})$.

While providing a powerful tool for the modeling of heterogeneous lattice structures with custom geometric parameters P, this approach is still limited to supporting only the constant values of T within each certain region of the structure. Note that this approach does not yet support stochastic lattices structures, and thus this work does not focus on the connectivity of stochastic topologies.

2.3 Connectivity issue

In beam-based topologies, the connectivity issue arises when there is no well-defined physical connection between the beams of two neighboring topologies. The connectivity issue affects the quality of the solid model of the lattice structure, as well as its manufacturability. Figure 7 sketches a scheme of a lattice structure with multiple topologies that have the connectivity issue.

This work focuses only on the connectivity of the beam-based topologies. To address this issue appropriately, a list of such topologies should be made. A substantial number of the beam-based topologies is inspired by the cubic crystal system in crystallography due to their ability to reinforce the structure in specific directions [33]. These topologies include simple cubic, body-centered cubic (BCC), face-centered cubic (FCC), as well as variations of these topologies such as self-supporting FCC without horizontal beams (S-FCC), BCC with additional 4 z-direction oriented beams (BCCz), FCC with additional 4 z-direction oriented beams (FCCz), S-FCCz, face- and body-centered cubic (FBCC), S-FBCC, and S-FBCCz [21]. Any of these topologies can be combined within a lattice structure without connectivity issues given the parallel translation of unit cells within it.

All the topologies inspired by the metal crystal structure which are listed above share the same cubic shape of their unit cell, as well as at least 4 common nodes. Thus, the connectivity of these topologies can be efficiently achieved.

However, countless other beam-based topologies that are not inspired by crystallography exist. Among the topologies that are extensively used in AM, there are the diamond, rhombicuboctahedron, truncated cube, and truncated cuboctahedron topologies. All of these except for the diamond topology are normally able to parallel transition from one to another without significant connectivity issues. The diamond topology is not plane symmetrical, i.e. it cannot be obtained by mirroring a subset of that topology about a plane. This effect limits the application of the diamond topology in lattice structures with multiple topologies.

The transition of unit cells with different topologies is not limited to parallel. For example, assigning BCC and FCC topologies oriented in different directions in different regions of the same lattice has proven mimicking of the crystal structure damage-resisting properties [34].

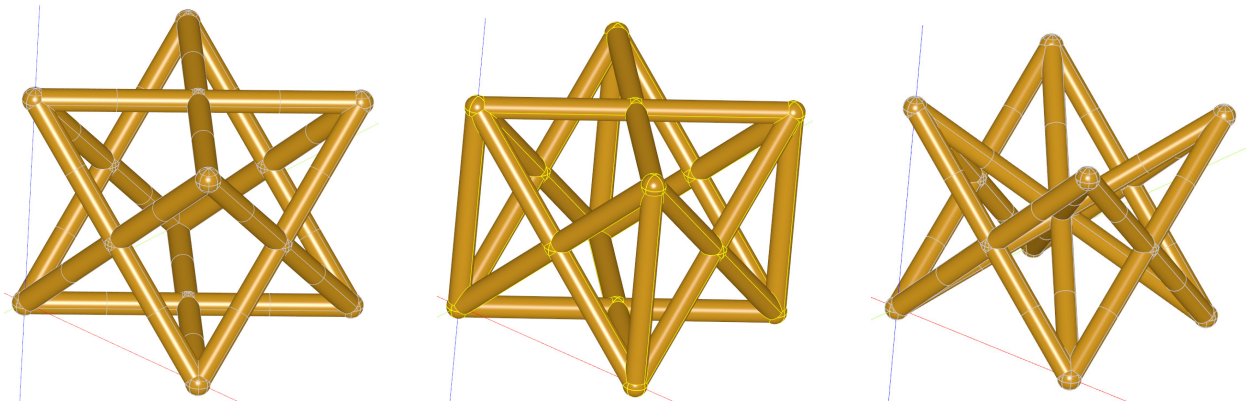

(a) FCC (b) FCCz (c) S-FBCC

Fig. 5: Various beam-based topologies inspired by the cubic crystal system supported by the F-rep approach [21]

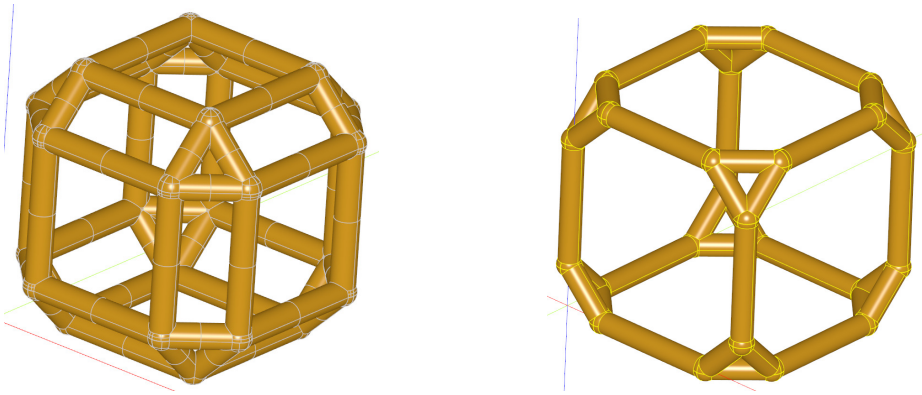

(a) Rhombicuboctahedron (b) Truncated cube

Fig. 6: Additional beam-based topologies supported by the F-rep approach [21] that are based on truncated polyhedrons

The connectivity issue, in this case, is often mitigated by introducing additional beams between the unmatched nodes in the transition plane for support [35]. However, these additional beams in the transition region can affect the mechanical properties that arise in it, thus making the outcome of the design process less predictable. In particular, it has been found that the mechanical properties in homogeneous lattice structures are easily predictable by various techniques such as the homogenization technique [36]. On the contrary, the connectivity region between various topologies is greatly affected by the geometric properties of the transition region which is more difficult to predict if stochastic [37].

3 THE PROPOSED FUNCTION REPRESENTATION APPROACH

Multiple commercial software packages that can model heterogeneous lattice structures exist. Many of those have been extensively reviewed in the literature [15, 16]. One of the most notable examples of such a tool is nTopology [38], which allows the modeling of highly complex lattice structures with heterogeneous parameters. However, the only geometric parameter that is allowed to be controlled in the majority of such tools is the thickness of the lattice. Moreover, there are not many open-source geometric modeling tools that would be able to model such complex shapes, while the ability to extend the software with additional functionality is of the essence. Thus, it is proposed to extend the F-rep approach described in section 2.2 to implement the connectivity of multiple topologies within the same lattice structure. The

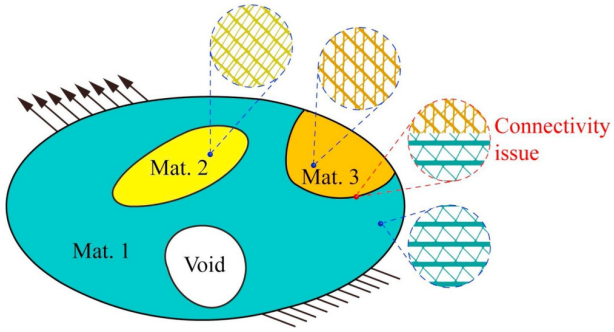

Fig. 7: A schematic of a lattice structure with multiple topologies [32] (Permission to reprint from Elsevier © 2020)

advantages of this approach include:

- Its ability to model a large amount of beam-based topologies.
- Its ability to extend the number of supported topologies by defining a custom function T that defines its skeletal graphs.
- Its support for defining a custom distribution of geometric parameters by providing control over the function P that defines them.
- Its ability to control geometric modeling parameters other than the thickness of the beam such as, for example, the shape of the beam cross-section. This is one of the key differences between this approach and other alternative approaches.
- Its release as a software prototype in the form of a free and open-source tool [31], which allows further improvements of the software.

3.1 Connectivity of beam-based topologies by the transition plane

A special case of topology transition at certain angles can be supported by the proposed approach. It is proposed to define the transition between the beam-based topologies by a transition plane. Since it is proposed to utilize the F-rep framework described in section 2.2, this transition plane is ought to be defined as a function.

Consider two topologies the skeletal graphs T_1 and T_2 for which are known. The transition plane $\mathcal{P}$ between them is a plane of the scalar form

$$\mathcal{P}(\mathbf{X}) : a_t(x-x_{0t})+b_t(y-y_{0t})+c_t(z-z_{0t})=0, \quad (7)$$

where a_t, b_t, and c_t are the components of the normal vector $\overrightarrow{n_t} = (a_t, b_t, c_t)$ of the transition plane, x_{0t}, y_{0t}, and z_{0t} are the coordinates of an arbitrary point on $\mathcal{P}$. In this case, the skeletal graph of the lattice structure with the two topologies that are separated by a transition plane $\mathcal{P}$ can be described as

$$T(\mathbf{X}) = \begin{bmatrix} \{T_1(\mathbf{X})|\mathcal{P}<0\}, \\ \{T_2(\mathbf{X})|\mathcal{P}>0\}, \\ \{(T_1 \cup T_2)(\mathbf{X})|\mathcal{P}=0\}, \end{bmatrix} \quad (8)$$

or, in a general case,

$$T(\mathbf{X}) = \begin{bmatrix} \{T_i(\mathbf{X})|\mathcal{P}_{ij}<0\} \\ \{T_j(\mathbf{X})|\mathcal{P}_{ij}>0\} \\ \{(T_i \cup T_j)(\mathbf{X})|\mathcal{P}_{ij}=0\} \end{bmatrix} \quad \forall i,j \in [1,...,N], \quad (9)$$

where $\mathcal{P}_{ij}$ is the transition plane between topologies T_i and T_j, N is the total number of regions with different topologies. Note that $\mathcal{P}_{ij} = -\mathcal{P}_{ji}$ is assumed to account for the change of the direction of a normal vector for each corresponding transition plane.

As an example, consider a lattice structure consisting of two topologies T_1 and T_2 which are oriented as sketched in Fig. 8. Let T_1 be a beam-based topology with a cubic unit cell with the side u_1. Let the transition plane $\mathcal{P}$ between them be defined as follows:

$$\mathcal{P}(\mathbf{X}) : x + z - pu_1 = 0, \quad (10)$$

where u_1 is the side of the cubic unit cell with the T_1 topology and p is the number of unit cells between the origin and the transition plane along the x-axis. In this case, the normal vector $\overrightarrow{n_t}$ of the transition plane $\mathcal{P}$ forms $45°$ with the positive direction of the x-axis. The T_2 topology has a cuboid shape of its unit cell with the dimensions of u_2, u_1, and u_2 in the x_2, y_2, and z_2 directions, respectively, where $u_2 = u_1/\sqrt{2}$. $\mathbf{X}_2 = (x_2, y_2, z_2)^\intercal$ is obtained by the Euclidean plane transformation of rotation as $\mathbf{X}_2 = R\mathbf{X}_1 = R\mathbf{X}$ where R is the rotation matrix defined as

$$R = \frac{\sqrt{2}}{2}\begin{bmatrix} 1 & 0 & 1 \\ 0 & \sqrt{2} & 0 \\ -1 & 0 & 1 \end{bmatrix}. \quad (11)$$

Note that the additional translation matrix is optional since T_2 is not defined for $\mathcal{P} < 0$.

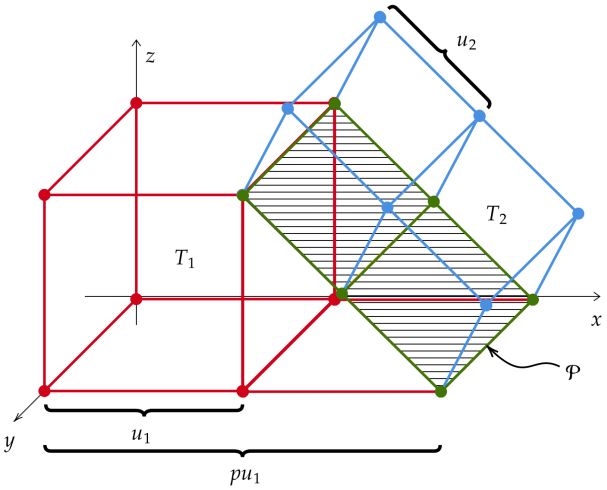

Fig. 8: A diagram of two topologies transitioning in a plane

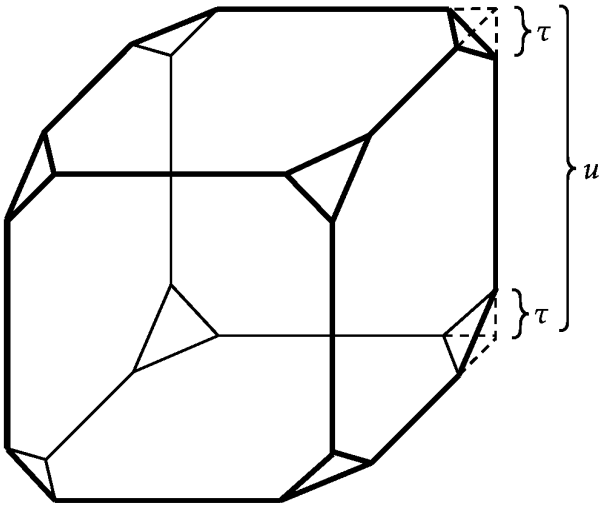

Fig. 9: A skeletal graph of the truncated cube topology with the unit cell size u and the truncation τ

3.2 Controllable truncation as a means to achieve topology transition

Some topologies have an optional truncation parameter required to fully define their skeletal graph T. For example, the rhombicuboctahedron (Fig. 6a) and the truncated cube (Fig. 6b) can have an additional truncation parameter τ that can be defined by the function P that defines geometric parameters.

The strict definition of many truncated polyhedrons assumes that every edge in them has equal length. Thus, the truncation in the truncated polyhedrons is considered to be defined. This work, however, steps back from the strict definitions of truncated polyhedrons. Consider a skeletal graph T of the truncated cube topology with the unit cell size u sketched in Fig. 9. The skeletal graph is defined according to the F-rep principles [21] as follows:

$$
T(\mathbf{X}): \left[\begin{array}{l}
x \in \{0,u\}, \left[\begin{array}{c} -y+\tau=z, \\ y-u+\tau=z, \\ y=z-u+\tau, \\ -y+u=z-u+\tau; \end{array}\right. \\
y \in \{0,u\}, \left[\begin{array}{c} -x+\tau=z, \\ x-u+\tau=z, \\ x=z-u+\tau, \\ x-u+\tau=-z+u; \end{array}\right. \\
z \in \{0,u\}, \left[\begin{array}{c} -x+\tau=y, \\ x-u+\tau=y, \\ x=y-u+\tau, \\ -x+u=y-u+\tau; \end{array}\right. \\
x \in [\tau, u-\tau], \left[\begin{array}{l} x \in \{0,u\}, \\ z \in \{0,u\}; \end{array}\right. \\
y \in [\tau, u-\tau], \left[\begin{array}{l} x \in \{0,u\}, \\ z \in \{0,u\}; \end{array}\right. \\
z \in [\tau, u-\tau], \left[\begin{array}{l} x \in \{0,u\}, \\ y \in \{0,u\}. \end{array}\right.
\end{array}\right. \tag{12}
$$

Here, the first 3 subsystems of equations correspond to the line segments that define the truncated faces and the other 3 subsystems of equations correspond to the edges of the cube.

The truncated cube, if defined as an Archimedean solid, assumes that τ is defined in such a way that every edge has an equal length. Thus

$$u = 2\tau + \sqrt{2}\tau \tag{13}$$

or

$$\tau = \frac{u}{2+\sqrt{2}}. \tag{14}$$

This work assumes that the truncation can take any real value in range $\tau \in [0, u/2]$, or for simplicity, between 0% and 100%.

Observe that in the two extreme cases when the value of τ takes 0 or $u/2$, Eqn. (12) that defines the truncated

cube illustrated in Fig. 6b, it converges to the simple cubic topology that is defined as

$$T(\mathbf{X}): \begin{bmatrix} x \in \{0,u\}, y \in \{0,u\}, \\ y \in \{0,u\}, z \in \{0,u\}, \\ x \in \{0,u\}, z \in \{0,u\} \end{bmatrix} \quad (15)$$

and to the cuboctahedron topology, respectively. This effect is known as the *complete quasitruncation*. Equation (12) and Eqn. (15) are defined on $x, y, z \in [0, u]$.

The approach is similarly applied to the rhombicuboctahedron topology. In the two extreme complete quasitruncation cases when the value of τ takes 0 or $u/2$, the rhombicuboctahedron topology converges to the simple cubic topology and the octahedron topology, respectively.

By considering the truncation τ as a variable instead of a constant, the proposed approach can achieve the transition of one topology T_1 into another topology T_2 by defining the function P that defines the geometric parameters. Note that the skeletal graph is different for any two different values of truncation $\tau \in [0, u/2]$. This effect blurs the differences between defining the geometric parameters with the function P and defining the topology with the function T.

4 IMPLEMENTATION

It was decided to extend the functionality of a previously developed implementation of the described F-rep approach [21, 31]. This approach is discussed in detail in section 2.2 and its framework is described by Eqn. (5). However, the implementation has only supported the variation of geometric parameters P and not the variation of topologies T. Thus, adjustments to the developed tool needed to be made.

The developed tool is based on Cadquery [39] with the Open CASCADE Technology (OCCT) [40] GMK. This allows the implementation of the same software development practices as in the previous work. Moreover, the software prototype developed this way remains cross-platform, thus enhancing the flexibility and applicability of the software.

4.1 Connectivity of beam-based topologies by the transition plane

As described in section 3.1, it is possible to achieve the transition of topology T_1 into topology T_2 by defining the transition plane $\mathcal{P}$ with an arbitrary position and orientation. This also enables support for non-cubic unit cells as one of the topologies may have the form of a cuboid.

As an example of such topology transition, consider a heterogeneous lattice structure with a total size of $37.5 \times 37.5 \times 37.5$ mm^3 which consists of topologies T_1 and T_2. Let T_1 and T_2 transition in the transition plane $\mathcal{P}$ defined as

$$\mathcal{P}(\mathbf{X}): x + z - 37.5 = 0, \quad (16)$$

so that the normal vector of $\mathcal{P}$ forms $45°$ with the positive direction of the x-axis. Let the topology T_1 correspond to the cubic FCC with the unit cell size of $u_1 = 3.75$ mm and the topology T_2 correspond to the cuboid BCC with the transition plane. Figure 10 illustrates the transition in detail. In this case, $u_2 = u_1/\sqrt{2} \cong 2.66$ mm. The connectivity issue in this case is resolved as the nodes of the two topologies are continuously connected in the transition plane.

According to the framework, after the definition of the topology T, the geometric parameters P are needed to be defined. The beams of the topologies in Fig. 10 are set to have the diameter $d = 0.7$ mm and the node diameter is set to $D = 0.75$ mm.

4.2 Controllable truncation as a means to achieve topology transition

As described in section 3.2, it is possible to achieve the transition of topology T by controlling other geometric parameters P such as the truncation τ of topologies that are based on the truncated polyhedrons. This can be done by defining $P(\mathbf{X}) : \tau(\mathbf{X})$.

As an example of such topology transition, consider a $10 \times 10 \times 10$ lattice structure with the truncated cube topology with the unit cell size $u = 10$ mm. Let the truncation τ of the truncated cube topology linearly change from $\tau_{\text{min}} = 0$ (0%) to $\tau_{\text{max}} = u/2 = 5$ mm (100%), i.e.

$$P(\mathbf{X}) : \tau(z) = z, \quad (17)$$

where $z \in [0, 1]$ is the variable corresponding to the z-axis. In this approach, $z \in [0, 1]$ is mapped to the actual coordinate $z_a \in [1, N_z]$ with $z_a \in \mathbb{N}^+$. The beam diameter is set to 1 mm and the node diameter is set to 1.05 mm. The resulting heterogeneous lattice structure is illustrated in Fig. 11. Note that at $z = 0$ the topology T that is described by Eqn. (12) converges to the simple cubic topology defined by Eqn. (15), and at $z = 1$ it converges to the cuboctahedron topology. The approach allows simultaneous control over different geometric parameters in different directions. In this example, the beam thickness is an

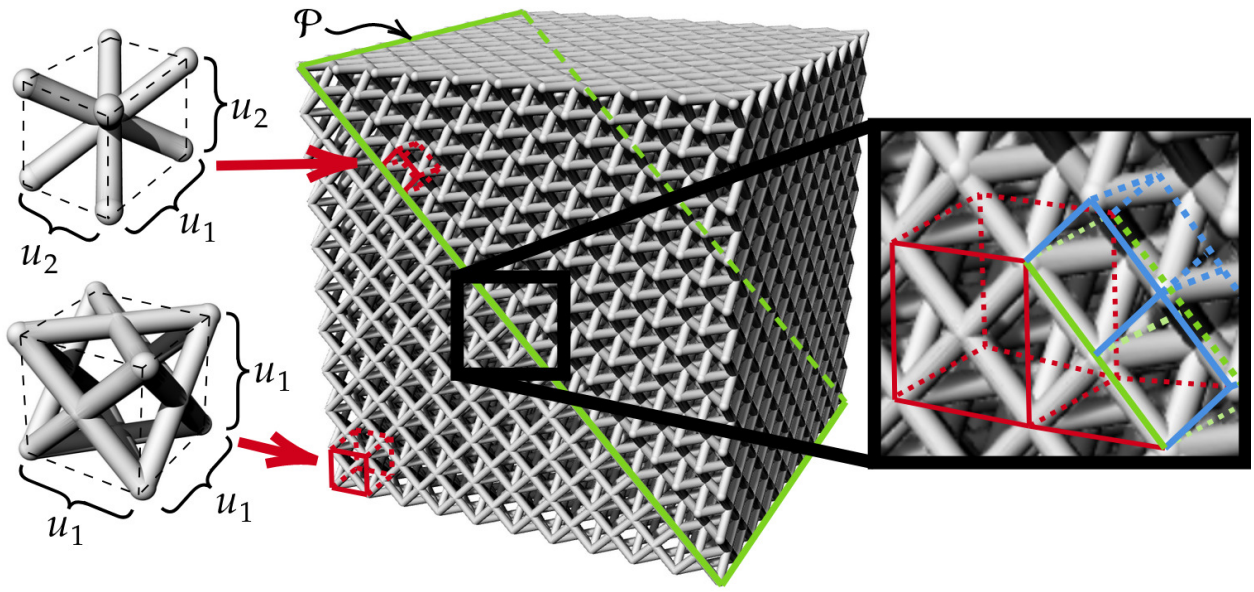

Fig. 10: The transition between the FCC topology with the cubic unit cell to the BCC topology with the cuboid unit cell along the transition plane $\mathcal{P}$. Note that the BCC topology is rotated $45°$.

additional parameter that linearly increases from 0.5 mm on the left and 5.0 mm on the right similarly to the truncation. Note that the lattice nodes have a diameter larger that the diameter of the beams and is set to linearly increase from 0.55 mm to 5.5 mm.

The truncation can be one of the potential output parameters of a topology optimization algorithm. For example, different regions of the lattice can be assigned a different truncation depending on whether the region is subject to bending-, compression-, or tension loads [41]. Additionally, since the control over the truncation allows a smooth and continuous transition between topologies, this approach can find its application in lattice embedding [42].

The estimation of mechanical properties in the lattice transition region can be more accurate due to the lack of stochastic geometric parameters.

Another example of a topology that can support the truncation-based topology transition is the rhombicuboctahedron topology. Consider a $10 \times 10 \times 10$ lattice structure with the rhombicuboctahedron topology with the unit cell size $u = 10$ mm. Let the truncation τ of the rhombicuboctahedron topology linearly change similarly to the previous example according to Eqn. (17). Similarly, the beam diameter is set to linearly increase from left to right. The resulting heterogeneous lattice structure is illustrated in Fig. 12. Note that at $z = 0$ the topology T described converges to the simple cubic topology defined, and at $z = 1$ it converges to the octahedron topology.

4.3 Performance analysis

The performance testing of the implemented approach was performed on a machine equipped with the AMD Ryzen™ 7 3700X central processing unit (CPU) with a 3.20 GHz of clock rate, the NVIDIA® GeForce® RTX 2070 Super graphics processing unit (GPU) with 8 GB of memory, 16 GB of random-access memory (RAM), a solid-state drive (SSD) and the Linux operating system. The modeling precision is customizable and can be set from the software settings. In this work, the modeling precision was set to be 0.1 mm. The performance of the developed approach when applied to some of the covered examples is listed in Table 1.

The previously developed software prototype supports the export of the resulting solid models into a stereolithography (STL) file encoded with the American Standard Code for Information Interchange (ASCII), and a STEP file defined by the ISO 10303-21 standard [43].

The manufacturability of the lattice is also an important aspect to consider when analyzing the resulting models [44]. The manufacturability check is run on the resulting STL models using the Preform 3D printing software [45].

It was decided to run the manufacturability checks for the transition plane connectivity similar to the example shown in Fig. 10 with all combinations of topologies

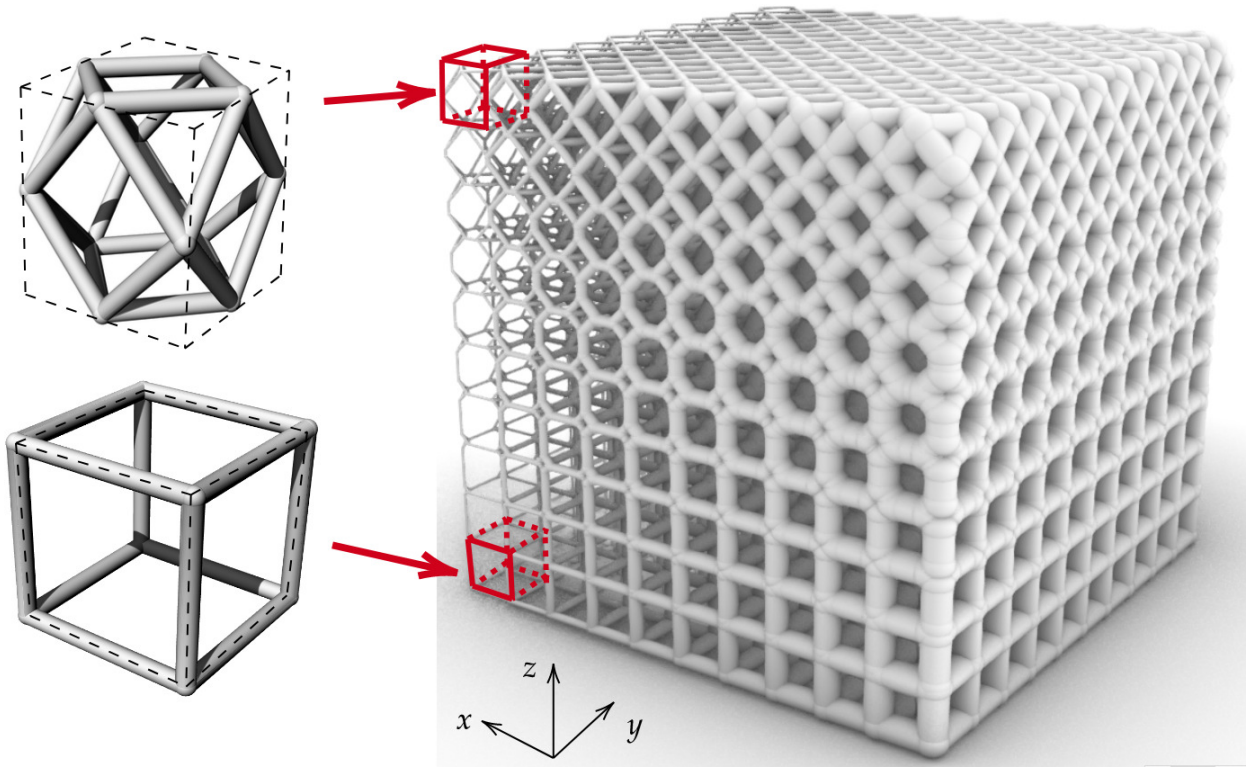

Fig. 11: A heterogeneous lattice structure with the topology based on a truncated cube with the truncation parameter τ varying along the z-axis. The topology converges to the simple cubic at the bottom and the cuboctahedron topology shifted to half of the unit cell size at the top. The thickness of the beams is linearly varying along the x-axis.

Lattice	CPU usage range, %	Generation time, min
Figure 10	40.9–101.3	19.76
Figure 11	43.5–102.1	34.97
Figure 12	45.7–106.8	37.62

Table 1: The performance metrics of the geometric modeling with the proposed approach

that are inspired by the crystal metal structure and that are listed in Fig. 5. Also, the same manufacturability checks have been performed for the truncation-based topology transition. The basic manufacturability checks within the software have been successfully passed.

Moreover, a case with multiple transitions of topologies was decided to be manufactured with the Formlabs Form 2 stereolithography 3D printer [46]. Stereolithography 3D printers allow highly accurate AM with a smooth finish [47]. The material was chosen to be Formlabs Elastic 50A [48]. It was decided to have 5 layers of FCC and 5 layers of BCC each with an equal layer thickness and oriented at 45° to the horizontal plane as illustrated in Fig. 13a. The FCC unit cell is cubic, and its size is set to $u_1 = 3.75$ mm. The BCC unit cell is cuboid and according to the framework described in section 3.1 and Fig. 8, its smaller side is $u_2 = u_1/\sqrt{2} \approx 2.65$ mm. The beam diameter for both topologies is set to $d = 0.7$ mm and the node diameter is set to $D = 0.75$ mm. Additional 3.75 mm thick plates were added at the bottom and at the top of the lattice structure to support it during the AM process. The resulting print is illustrated in Fig. 13b. Note that one of the plates is bent in an arc which can be explained by its shrinkage due to the residual stress occurring in it during the print, as this plate was the one attached to the printing platform [49].

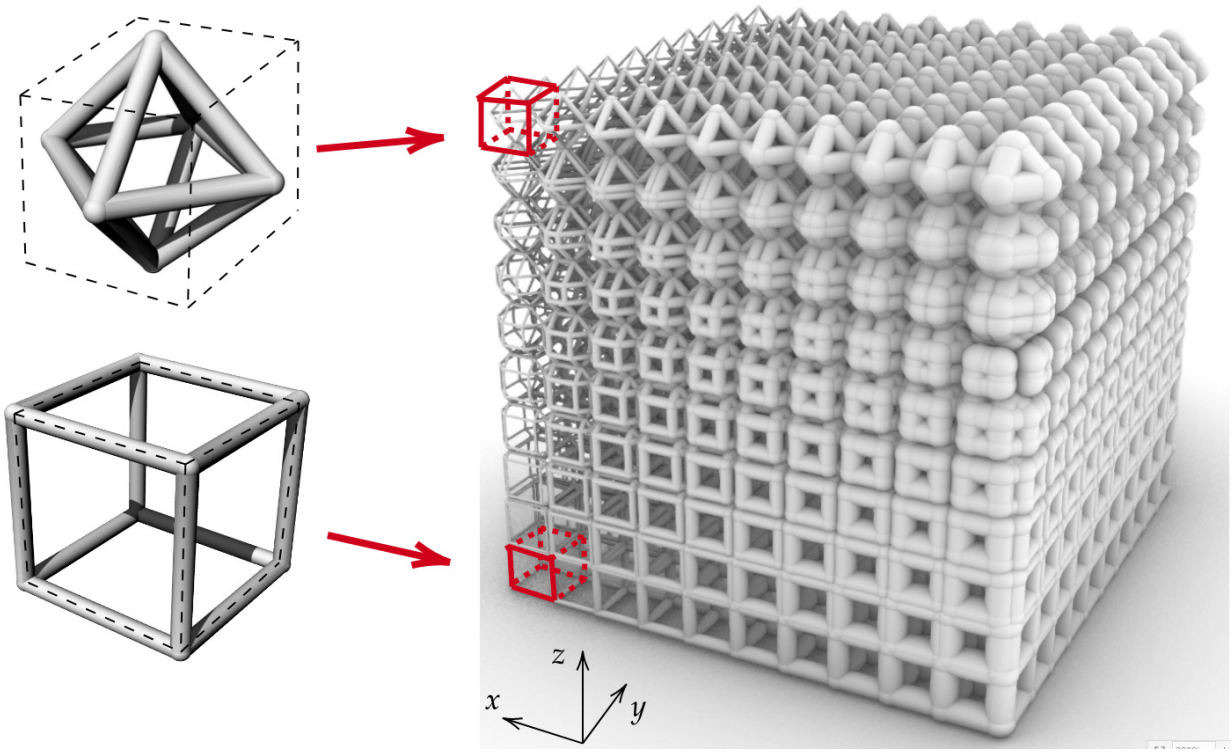

Fig. 12: A heterogeneous lattice structure with the topology based on a rhombicuboctahedron with the truncation parameter τ varying along the z-axis. The topology converges to the simple cubic at the bottom and the octahedron topology at the top. The thickness of the beams is linearly varying along the x-axis.

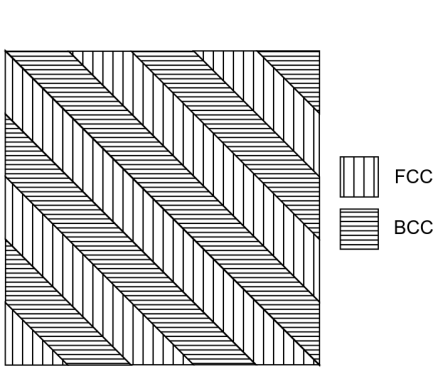

(a) The orientation of topologies for the manufacturability performance test

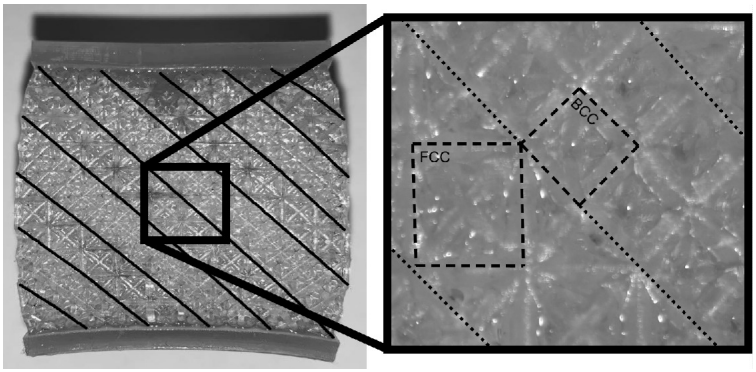

(b) The resulting print with a zoomed-in view on the topology transition region. In the zoomed-in view, the transition planes are marked with dotted lines and the instances of the FCC and BCC unit cells are marked with the dashed lines.

Fig. 13: A use-case showing the lattice transition with the proposed approach

5 CONCLUSION AND FUTURE RESEARCH

This work provides a novel geometric modeling approach that allows the generation of lattice structures with multiple topologies. The topology transition based on the transition plane has been shown to enable cuboid unit cells. A novel approach for transforming a topology from one to another which is based on the variation of geometric parameters has been proposed and implemented in a software prototype. Several use cases of transition of topology by the variation of the truncation parameter

have been covered. These topology transformations have been implemented with a novel F-rep approach.

The integration in the design loop is proposed to be achieved by providing access and guidance to the design community and to a list of manufacturers utilizing which utilize lattice structures. The aerospace sector is of the sectors of industry that heavily relies on lightweight structures with unique thermophysical properties, and is thus proposed as a potential venue for exploration. The tool is released as a documented FOSS which should enhance the user experience and foster further agile development of the tool.

It is proposed to investigate the topology transition between TPMS-based topologies and the applicability of F-rep to this transition. While this topic has been of interest with several of successful implementations, there may be ways to improve the existing methods with the F-rep approaches. It is also important to find industrial use cases of extreme heterogeneity of lattice structures that could benefit from the proposed approach.

The diamond beam-based lattice structure is an example of a beam-based topology that does not have conventional nodes at the edges of its cubic unit cell. Moreover, the properties of such lattice depend on the orientation of the unit cells. It is proposed to investigate the application of the proposed approach to this topology. The software prototype that embeds the proposed approach has been developed according to the object-oriented programming principles, which enables further extension of the framework.

There is evidence that lattice structures with multiple topologies can possess unique properties. It is proposed to model geometrically complex lattice structures that would be challenging to manufacture with other existing means.

The future work is also proposed to focus on supporting multi-scale hierarchical lattice structures with the F-rep approach.

ACKNOWLEDGEMENTS

This research work is supported by National Sciences and Engineering Research Council of Canada Discovery Grant RGPIN-2018-05971.

REFERENCES

[1] Yang, S., Tang, Y., and Zhao, Y. F., 2015, "A new part consolidation method to embrace the design freedom of additive manufacturing," *Journal of Manufacturing Processes,* **20**, pp. 444–449.

[2] Lam, H. K., Ding, L., Cheng, T., and Zhou, H., 2019, "The impact of 3D printing implementation on stock returns: a contingent dynamic capabilities perspective," *International Journal of Operations & Production Management*.

[3] Noronha, J., Qian, M., Leary, M., Kyriakou, E., and Brandt, M., 2021, "Hollow-walled lattice materials by additive manufacturing: Design, manufacture, properties, applications and challenges," *Current Opinion in Solid State and Materials Science,* **25**(5), p. 100940.

[4] Queheillalt, D. T., and Wadley, H. N., 2005, "Cellular metal lattices with hollow trusses," *Acta Materialia,* **53**(2), pp. 303–313.

[5] Yazdi, M. S., Latifi Rostami, S., and Kolahdooz, A., 2016, "Optimization of geometrical parameters in a specific composite lattice structure using neural networks and abc algorithm," *Journal of Mechanical Science and Technology,* **30**(4), pp. 1763–1771.

[6] Chen, D., and Zheng, X., 2018, "Multi-material additive manufacturing of metamaterials with giant, tailorable negative poisson's ratios," *Scientific reports,* **8**(1), pp. 1–8.

[7] Maconachie, T., Leary, M., Lozanovski, B., Zhang, X., Qian, M., Faruque, O., and Brandt, M., 2019, "SLM lattice structures: Properties, performance, applications and challenges," *Materials & Design,* **183**, p. 108137.

[8] Aslan, B., and Yıldız, A. R., 2020, "Optimum design of automobile components using lattice structures for additive manufacturing," *Materials testing,* **62**(6), pp. 633–639.

[9] Kandil, K., Kaoua, S. A., Mesbah, A., Voznyak, Y., Zaïri, F., and Zaïri, F., 2021, "A novel bio-inspired hydrogel-based lattice structure to mechanically mimic human annulus fibrosus: A finite element study," *International Journal of Mechanical Sciences,* **211**, p. 106775.

[10] Dong, G., Tang, Y., and Zhao, Y. F., 2017, "A survey of modeling of lattice structures fabricated by additive manufacturing," *Journal of Mechanical Design,* **139**(10), p. 100906.

[11] Li, C., Lei, H., Zhang, Z., Zhang, X., Zhou, H., Wang, P., and Fang, D., 2020, "Architecture design of periodic truss-lattice cells for additive manufacturing," *Additive Manufacturing,* **34**, p. 101172.

[12] Liu, Y., Zhuo, S., Xiao, Y., Zheng, G., Dong, G., and Zhao, Y. F., 2020, "Rapid modeling and design optimization of multi-topology lattice structure based on unit-cell library," *Journal of Mechanical Design,* **142**(9), p. 091705.

[13] Hu, J., Luo, Y., and Liu, S., 2021, "Two-scale con-

current topology optimization method of hierarchical structures with self-connected multiple lattice-material domains," *Composite Structures,* **272**, p. 114224.

[14] Wei, N., Ye, H., Zhang, X., Li, J., and Sui, Y., 2022, "Topology optimization for design of hybrid lattice structures with multiple microstructure configurations," *Acta Mechanica Solida Sinica*, pp. 1–17.

[15] Letov, N., Velivela, P. T., Sun, S., and Zhao, Y. F., 2021, "Challenges and opportunities in geometric modeling of complex bio-inspired three-dimensional objects designed for additive manufacturing," *Journal of Mechanical Design,* **143**(12).

[16] Liu, Y., Zheng, G., Letov, N., and Zhao, Y. F., 2021, "A survey of modeling and optimization methods for multi-scale heterogeneous lattice structures," *Journal of Mechanical Design,* **143**(4).

[17] Tao, W., and Leu, M. C., 2016, "Design of lattice structure for additive manufacturing," In 2016 International Symposium on Flexible Automation (ISFA), IEEE, pp. 325–332.

[18] Velivela, P. T., Letov, N., Liu, Y., and Zhao, Y. F., 2021, "Application of domain integrated design methodology for bio-inspired design-a case study of suture pin design," *Proceedings of the Design Society,* **1**, pp. 487–496.

[19] Leonardi, F., Graziosi, S., Casati, R., Tamburrino, F., and Bordegoni, M., 2019, "Additive manufacturing of heterogeneous lattice structures: an experimental exploration," In Proceedings of the Design Society: International Conference on Engineering Design, Vol. 1, Cambridge University Press, pp. 669–678.

[20] Lu, Y., Cheng, L., Yang, Z., Li, J., and Zhu, H., 2020, "Relationship between the morphological, mechanical and permeability properties of porous bone scaffolds and the underlying microstructure," *PloS one,* **15**(9), p. e0238471.

[21] Letov, N., and Zhao, Y. F., 2022, "A geometric modeling framework to support the design of heterogeneous lattice structures with non-linearly varying geometry," *Journal of Computational Design and Engineering*, p. qwac076.

[22] Liu, Y., Zhou, M., Tang, Y., Zhao, Y., and Zheng, G., 2019, "Material-unit network for multi-material-property and multiscale components," *Computer-Aided Design and Applications,* **17**, pp. 547–560.

[23] Popov, D., Kuzminova, Y., Maltsev, E., Evlashin, S., Safonov, A., Akhatov, I., and Pasko, A., 2021, "Cad/cam system for additive manufacturing with a robust and efficient topology optimization algorithm based on the function representation," *Applied Sciences,* **11**(16), p. 7409.

[24] Al-Ketan, O., Lee, D.-W., Rowshan, R., and Al-Rub, R. K. A., 2020, "Functionally graded and multi-morphology sheet tpms lattices: Design, manufacturing, and mechanical properties," *Journal of the mechanical behavior of biomedical materials,* **102**, p. 103520.

[25] Ren, F., Zhang, C., Liao, W., Liu, T., Li, D., Shi, X., Jiang, W., Wang, C., Qi, J., Chen, Y., et al., 2021, "Transition boundaries and stiffness optimal design for multi-tpms lattices," *Materials & Design,* **210**, p. 110062.

[26] Savio, G., Meneghello, R., and Concheri, G., 2018, "Geometric modeling of lattice structures for additive manufacturing," *Rapid Prototyping Journal*.

[27] Lertthanasarn, J., 2021, "Hierarchical strengthening of polycrystal-inspired lattice materials," PhD Thesis, Imperial College London, London, UK, accessed April 16, 2022 `https://ethos.bl.uk/OrderDetails.do?uin=uk.bl.ethos.849669`.

[28] Letov, N., and Zhao, Y. F., 2020, "Volumetric cells: A framework for a bio-inspired geometric modelling method to support heterogeneous lattice structures," In Proceedings of the Design Society: DESIGN Conference, Vol. 1, Cambridge University Press, pp. 295–304.

[29] Pasko, A., Adzhiev, V., Sourin, A., and Savchenko, V., 1995, "Function representation in geometric modeling: concepts, implementation and applications," *The visual computer,* **11**(8), pp. 429–446.

[30] Kartasheva, E., Adzhiev, V., Comninos, P., Fryazinov, O., and Pasko, A., 2008, "An implicit complexes framework for heterogeneous objects modelling," In *Heterogeneous Objects Modelling and Applications*. Springer, pp. 1–41.

[31] Letov, N., 2022, jalovisko/LatticeQuery 0.1LQ, accessed August 30, 2022, `https://zenodo.org/record/6959068`.

[32] Liu, P., Kang, Z., and Luo, Y., 2020, "Two-scale concurrent topology optimization of lattice structures with connectable microstructures," *Additive Manufacturing,* **36**, p. 101427.

[33] Maskery, I., Hussey, A., Panesar, A., Aremu, A., Tuck, C., Ashcroft, I., and Hague, R., 2017, "An investigation into reinforced and functionally graded lattice structures," *Journal of Cellular Plastics,* **53**(2), pp. 151–165.

[34] Pham, M.-S., Liu, C., Todd, I., and Lertthanasarn, J., 2019, "Damage-tolerant architected materials inspired by crystal microstructure," *Nature,* **565**(7739), pp. 305–311.

[35] Lertthanasarn, J., Liu, C., and Pham, M.-S., 2021, "Influence of the base material on the mechanical behaviors of polycrystal-like meta-crystals," *Journal of Micromechanics and Molecular Physics*, p. 2150004.

[36] Somnic, J., and Jo, B. W., 2022, "Status and challenges in homogenization methods for lattice materials," *Materials,* **15**(2), p. 605.

[37] Wang, P., Casadei, F., Kang, S. H., and Bertoldi, K., 2015, "Locally resonant band gaps in periodic beam lattices by tuning connectivity," *Physical Review B,* **91**(2), p. 020103.

[38] nTopology, Inc. Next-Generation Engineering Design Software Online, accessed September 1, 2022, https://ntopology.com/.

[39] Urbańczyk, A., Wright, J., Cowden, D., Innovations Technology Solutions, Özderya, H. Y., Boyd, M., Agostini, B., Greminger, M., Buchanan, J., Cactrot, Huskier, de León Peque, M. S., Boin, P., Saville, W., Weissinger, B., Ruben, Nopria, Osterwood, C., Moeb, Kono, A., HLevering, Turner, W., Trhoň, A., Christoforo, G., Just-georgeb, Peterson, A., Grunichev, A., Gregg-Smith, A., Bernhard, and Anderson, D., 2021, CadQuery/cadquery: CadQuery 2.1. Repository, accessed February 7, 2022, https://github.com/CadQuery/cadquery/tree/2.1.

[40] Open Cascade S.A.S. Open Cascade – software development company. Online, accessed March 6, 2022, https://www.opencascade.com/.

[41] Alghamdi, A., Maconachie, T., Downing, D., Brandt, M., Qian, M., and Leary, M., 2020, "Effect of additive manufactured lattice defects on mechanical properties: an automated method for the enhancement of lattice geometry," *The International Journal of Advanced Manufacturing Technology,* **108**(3), pp. 957–971.

[42] Sanders, E., Pereira, A., and Paulino, G., 2021, "Optimal and continuous multilattice embedding," *Science Advances,* **7**(16), p. eabf4838.

[43] ISO 10303-21:2016, 2016, Industrial automation systems and integration — Product data representation and exchange – Part 21: Implementation methods: Clear text encoding of the exchange structure Standard, International Organization for Standardization, Geneva, CH, Mar. visited 2021-08-16.

[44] Zhang, Y., and Zhao, Y. F., 2022, "Hybrid sparse convolutional neural networks for predicting manufacturability of visual defects of laser powder bed fusion processes," *Journal of Manufacturing Systems,* **62**, pp. 835–845.

[45] Formlabs Inc. Preform 3D Printing Software. Online, accessed March 1, 2022, https://formlabs.com/software/#preform.

[46] Formlabs Inc. Form 2: Affordable Desktop SLA 3D Printer. Online, accessed March 11, 2022, https://formlabs.com/3d-printers/form-2.

[47] Bhattacharjee, N., Parra-Cabrera, C., Kim, Y. T., Kuo, A. P., and Folch, A., 2018, "Desktop-stereolithography 3D-printing of a poly (dimethylsiloxane)-based material with sylgard-184 properties," *Advanced materials,* **30**(22), p. 1800001.

[48] Formlabs Inc. Material data sheet. Elastic 50A. Online, accessed March 11, 2022, https://formlabs-media.formlabs.com/datasheets/2001420-TDS-ENUS-0.pdf.

[49] Milovanović, A., Milošević, M., Mladenović, G., Likozar, B., Čolić, K., and Mitrović, N., 2018, "Experimental dimensional accuracy analysis of reformer prototype model produced by FDM and SLA 3D printing technology," In *Experimental and numerical investigations in materials science and engineering*. Springer, pp. 84–95.